Supporting Information

Icosahedron-kernel defect in Pt_1Ag_x series bimetallic nanoclusters enhances photocatalytic hydrogen evolution

Dong Tan, ‡[a] Tengfei Ding, ‡[a] Kaidong Shen, ‡[a] Chang Xu,[a] Shan Jin,[b] Daqiao Hu,*[a] Song Sun*[a] and Manzhou Zhu*[a]

[a] Department of Chemistry and Centre for Atomic Engineering of Advanced Materials, Key Laboratory of Structure and Functional Regulation of Hybrid Materials of Ministry of Education, Anhui University, Hefei, Anhui 230601, China.

[b] Institutes of Physical Science and Information Technology, Anhui University, Hefei, Anhui 230601, China.

*E-mail: hudaqiao@ahu.edu.cn; suns@ustc.edu.cn; zmz@ahu.edu.cn

This Supplementary Information includes:

Supplementary Figures 1-27

Supplementary Tables 1-8

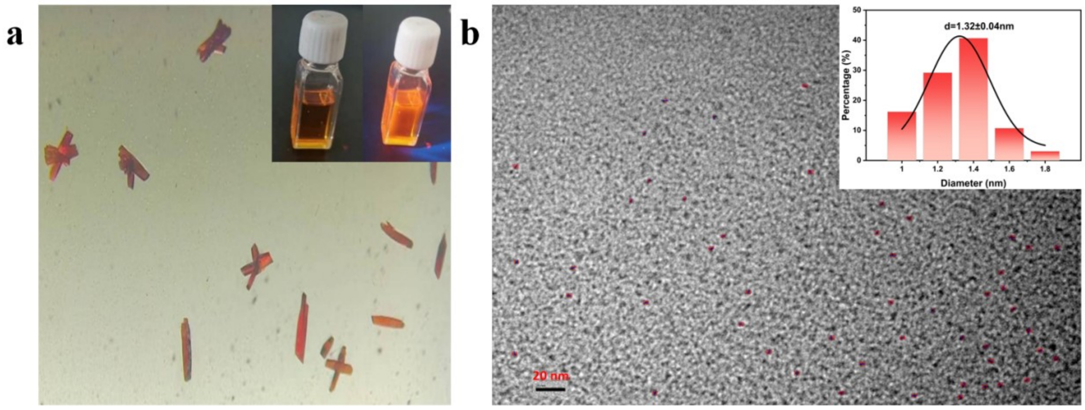

Supplementary Figure 1. (**a**) Crystal images of Pt_1Ag_{11}. Insert of Digital photographs of Pt_1Ag_{11} in CH_2Cl_2 under visible and UV lights. (**b**) Transmission electron microscope (TEM) images of Pt_1Ag_{11}. Insert of (b) the corresponding histogram of Pt_1Ag_{11}.

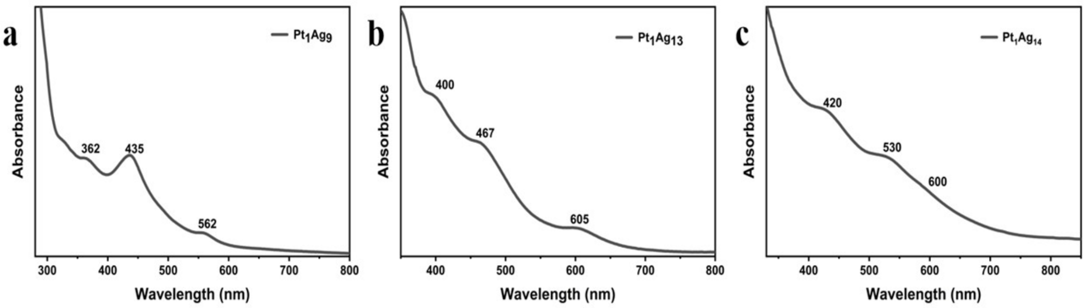

Supplementary Figure 2. UV/Vis spectra of Pt_1Ag_9 (**a**); Pt_1Ag_{13} (**b**); and Pt_1Ag_{14} (**c**) NCs in CH_2Cl_2 at room temperature.

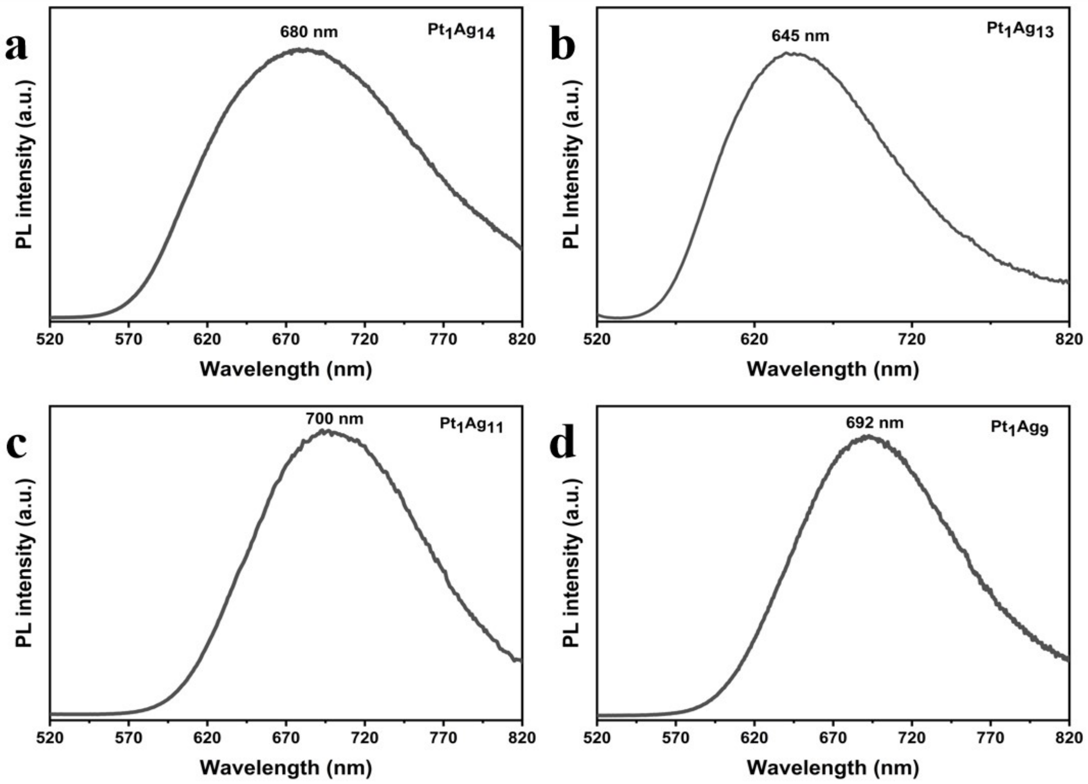

Supplementary Figure 3. Emission spectra of Pt_1Ag_{14} (**a**), Pt_1Ag_{13} (**b**), Pt_1Ag_{11} (**c**) and Pt_1Ag_9 (**d**) NCs in the solid state at room temperature.

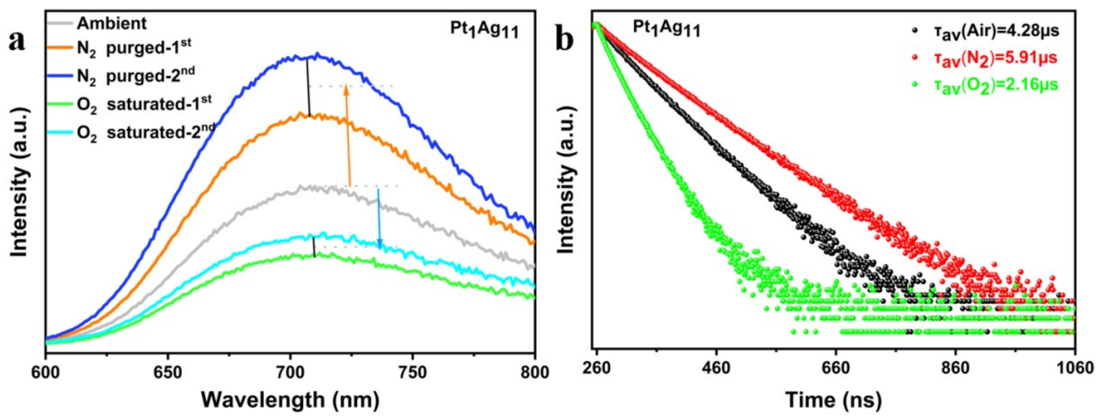

Supplementary Figure 4. (**a**) Comparison of the emission spectra of the Pt_1Ag_{11} under ambient condition (grey line), N_2-purged (pale red and purple lines), and O_2-saturated (pale green and pale blue lines) conditions; λ_{ex} = 460 nm. (**b**) Time-resolved PL decays of the Pt_1Ag_{11} in the solid state.

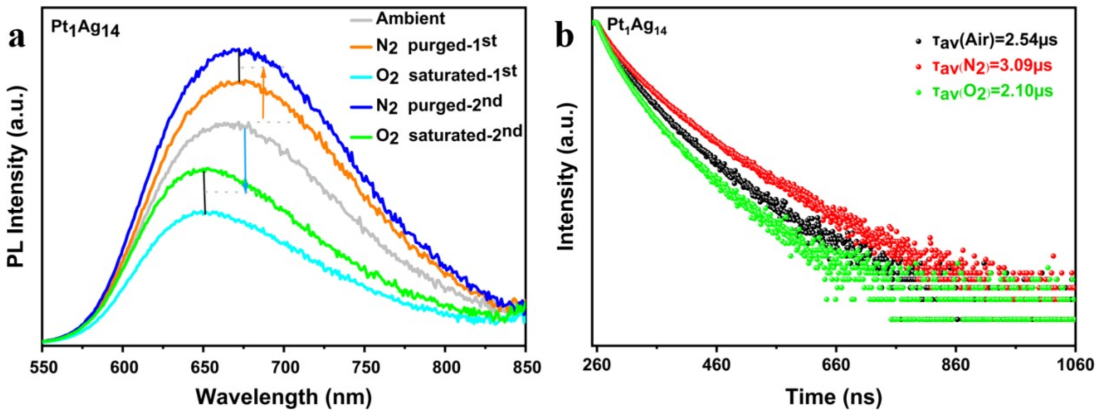

Supplementary Figure 5. (**a**) Comparison of the emission spectra of the Pt_1Ag_{14} under ambient condition (grey line), N_2-purged (pale red and purple lines), and O_2-saturated (pale green and pale blue lines) conditions; λ_{ex} = 460 nm. (**b**) Time-resolved PL decays of the Pt_1Ag_{14} in the solid state.

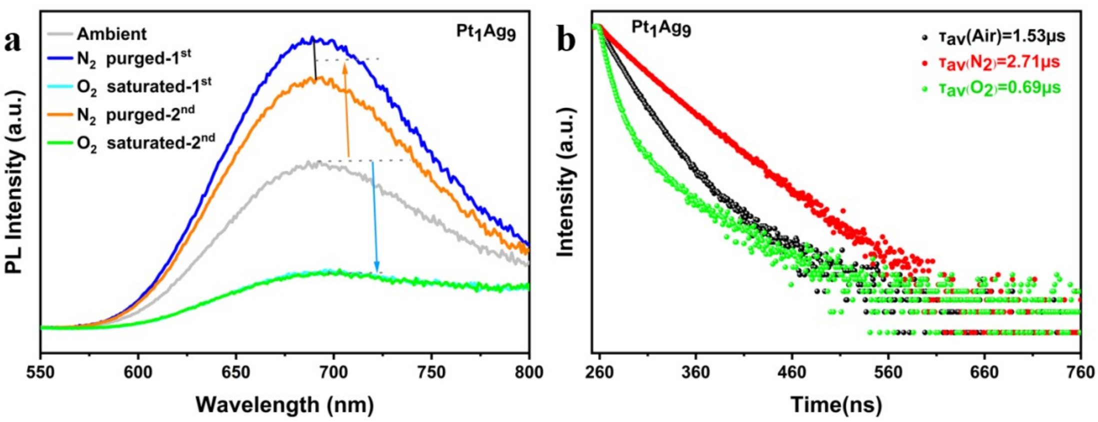

Supplementary Figure 6. (**a**) Comparison of the emission spectra of the Pt_1Ag_9 under ambient condition (grey line), N_2-purged (pale red and purple lines), and O_2-saturated (pale green and pale blue lines) conditions; λ_{ex} = 460 nm. (**b**) Time-resolved PL decays of the Pt_1Ag_9 in the solid state.

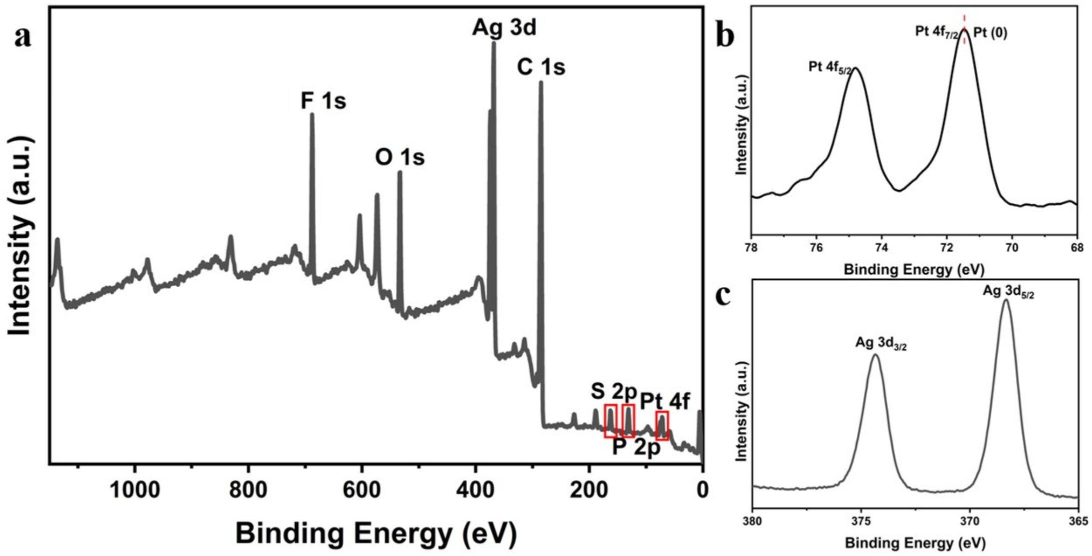

Supplementary Figure 7. (**a**) X-ray photoelectron spectroscopy (XPS) spectrum of the Pt_1Ag_{11}. XPS of Pt *4f* (**b**), Ag *3d* (**c**) in Pt_1Ag_{11}.

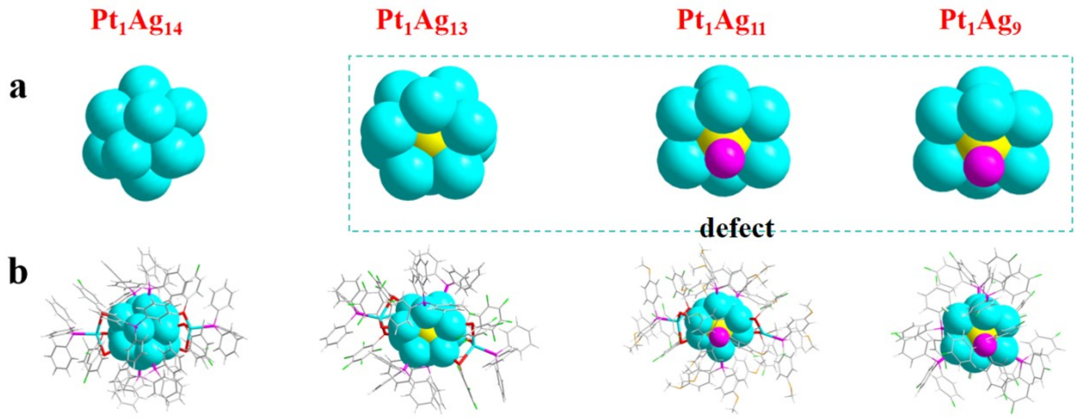

Supplementary Figure 8. (**a**) kernel (**b**) overall structure. The space-filling model of the Pt_1Ag_x NCs (x = 9, 11, 13, 14).

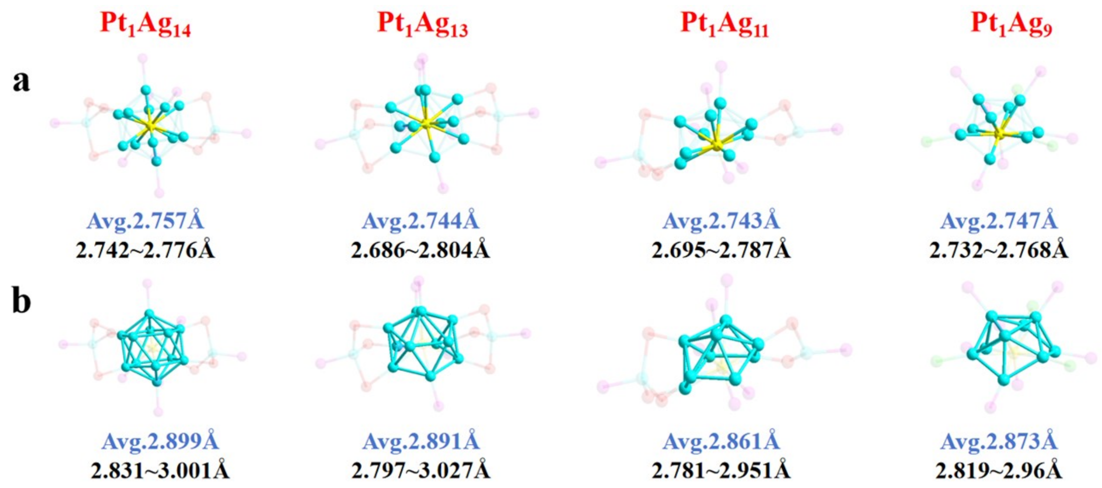

Supplementary Figure 9. (**a**) Comparison of lengths of Pt-Ag. (**b**) Comparison of the lengths Ag-Ag. The compared bonds are highlighted.

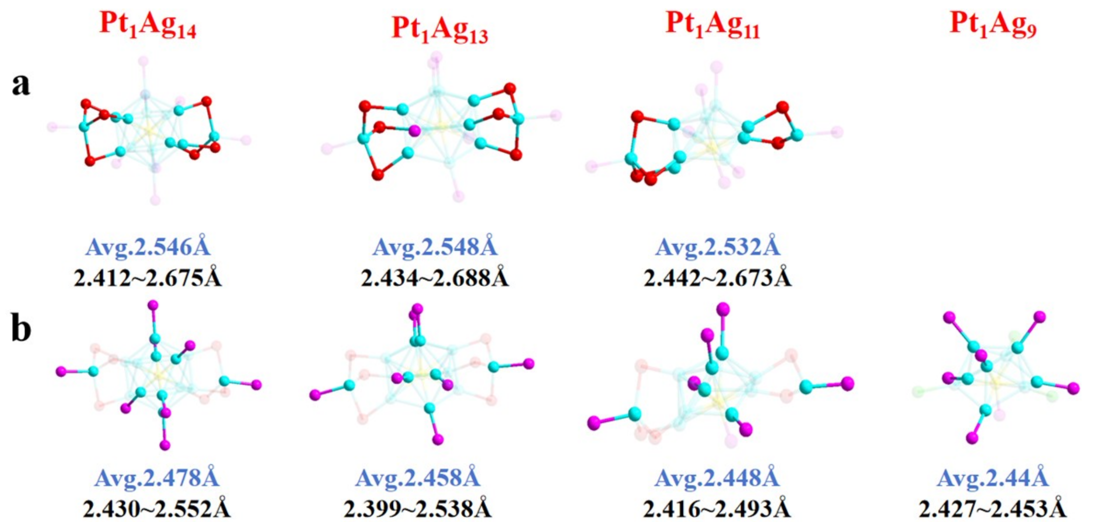

Supplementary Figure 10. (**a**) Comparison of lengths of Ag-S. (**b**) Comparison of lengths of Ag-P. The compared bonds are highlighted.

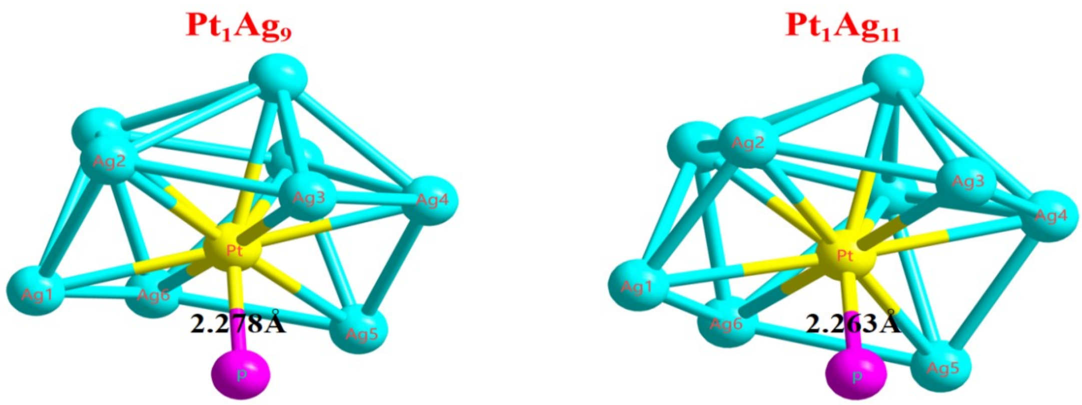

Supplementary Figure 11. Comparison of Pt-P bond length of Pt_1Ag_9 and Pt_1Ag_{11} NCs.

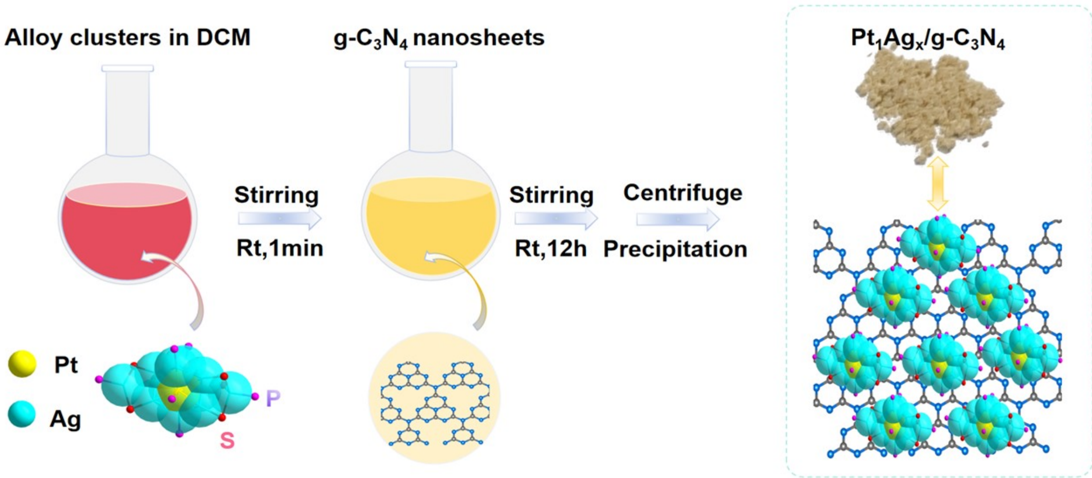

Scheme S1. Schematic illustration for the preparation of Pt_1Ag_x/g-C_3N_4 (x = 9, 11, 13, 14).

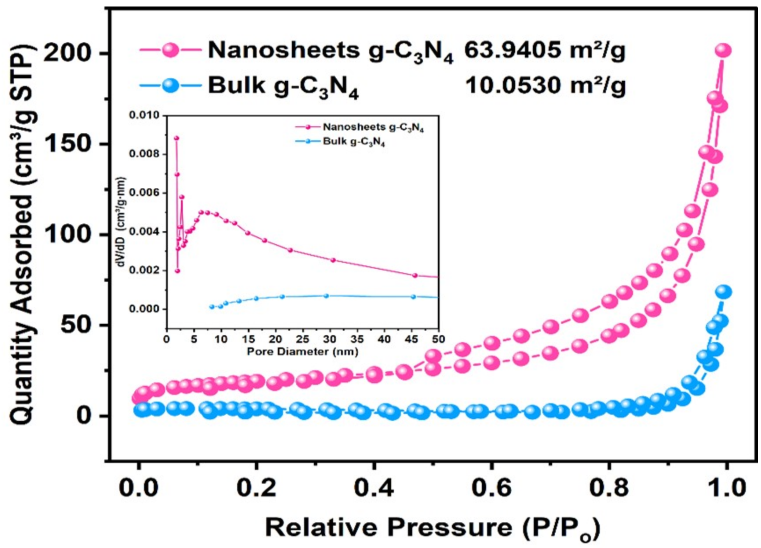

Supplementary Figure 12. N_2 sorption isotherms of bulk and nanosheets g-C_3N_4 at 125℃, the insert is the corresponding pore size distributions.

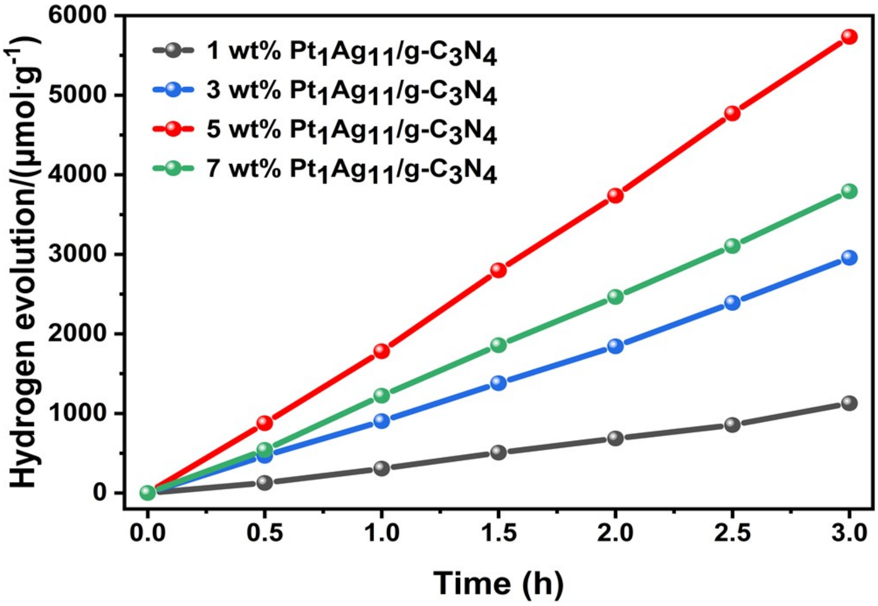

Supplementary Figure 13. Photocatalytic H_2 production of the M wt% $Pt_1Ag_{11}/g\text{-}C_3N_4$ (M=1, 3, 5, and 7mg).

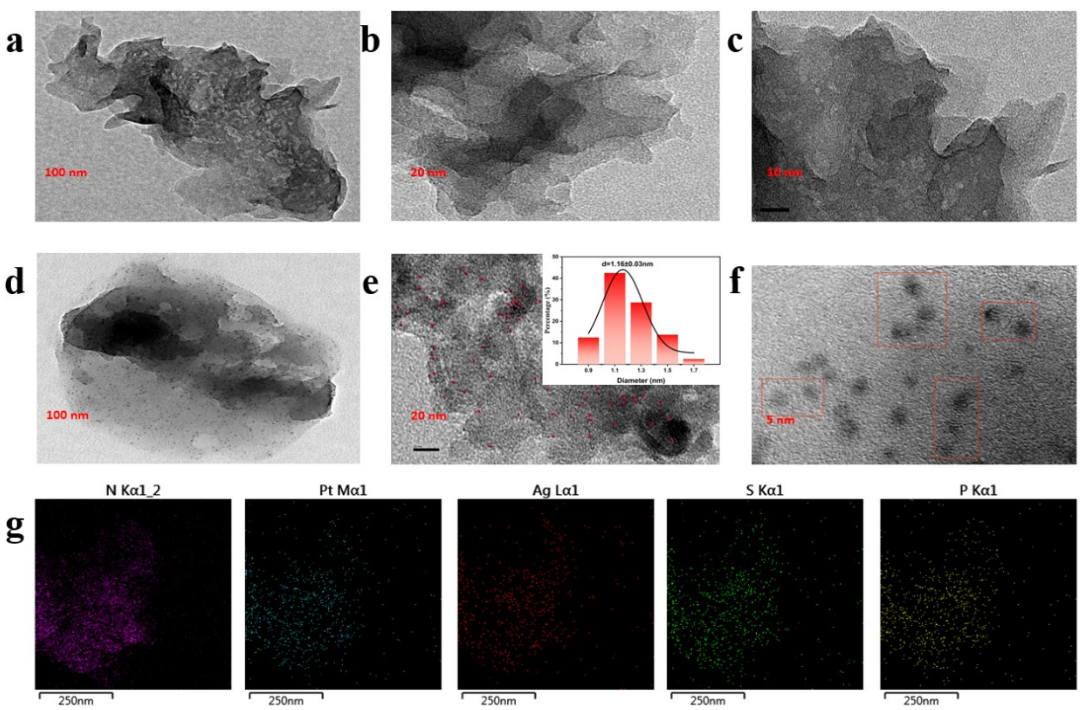

Supplementary Figure 14. TEM images of (**a-c**) synthesized $g\text{-}C_3N_4$, (**d-f**) $Pt_1Ag_{11}/g\text{-}C_3N_4$ and (**g**) the corresponding EDX mapping of N, Pt, Ag, S and P elements for $Pt_1Ag_{11}/g\text{-}C_3N_4$.·

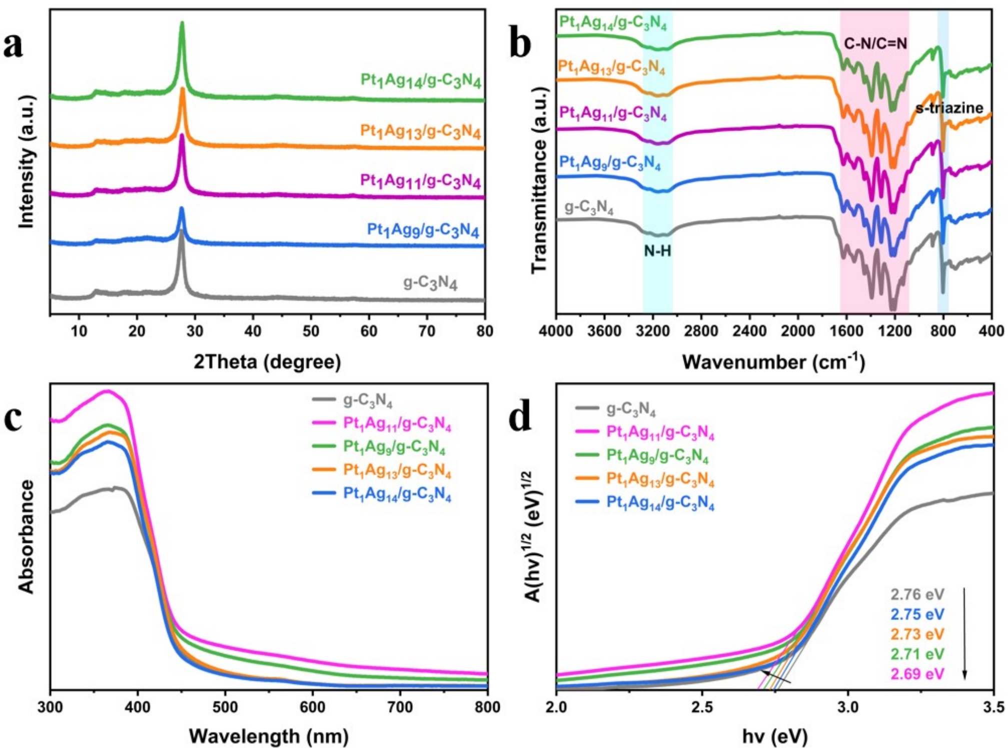

Supplementary Figure 15. (**a**) Powder XRD patterns; (**b**) FTIR spectra, (**c**) The UV-vis diffuse reflection spectroscopy (DRS), (**d**) Tauc plot of synthesized $g-C_3N_4$ and $Pt_1Ag_x/g-C_3N_4$ (x = 9, 11, 13 and 14).

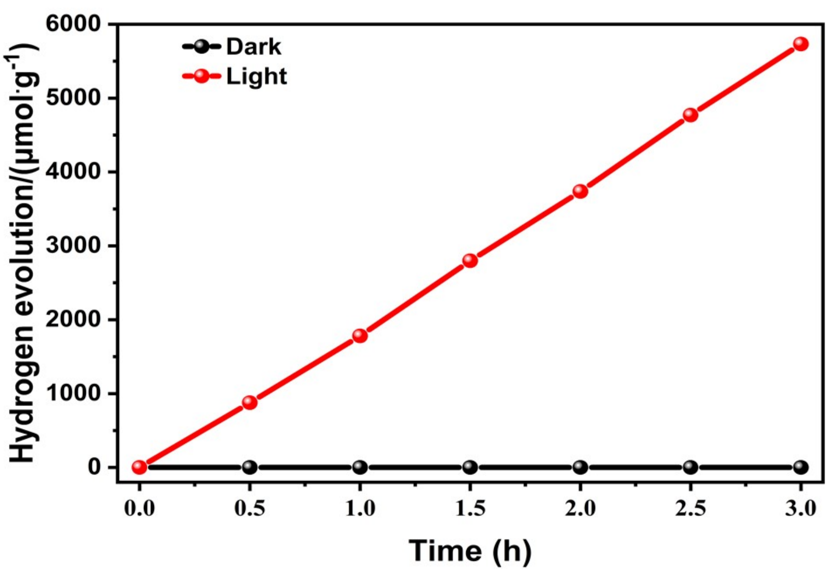

Supplementary Figure 16. Photocatalytic H_2 production of $Pt_1Ag_{11}/g-C_3N_4$ (light on or off).

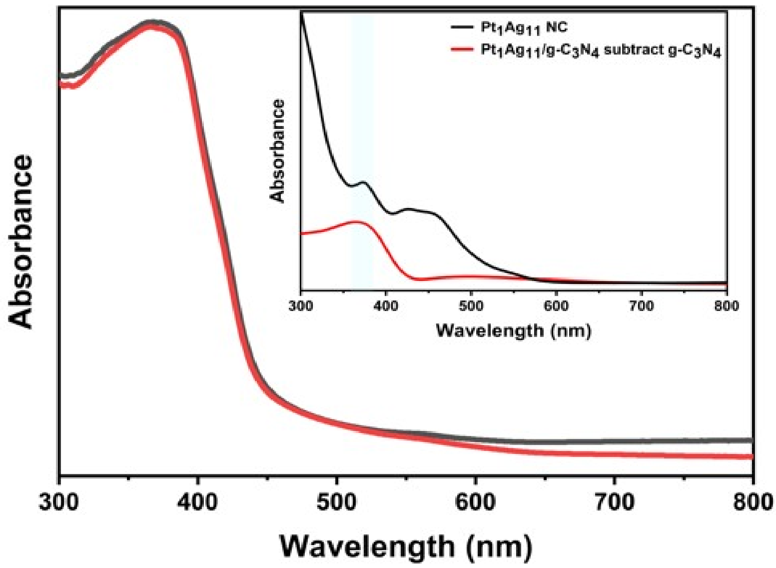

Supplementary Figure 17. The UV-vis diffuse reflection spectroscopy of Pt_1Ag_{11}/g-C_3N_4 before (black line) and after (red line) reactions. (inset: UV-vis spectra of Pt_1Ag_{11} loaded on or encapsulated into g-C_3N_4 by subtracting the spectrum of g-C_3N_4 from Pt_1Ag_{11}/g-C_3N_4.)

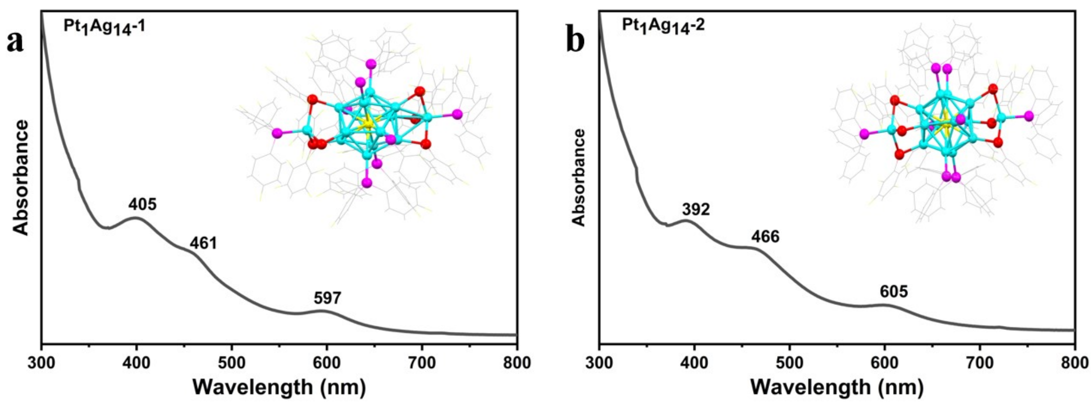

Supplementary Figure 18. The UV-vis absorption spectra of (**a**) Pt_1Ag_{14}-1, (**b**) Pt_1Ag_{14}-2 (inset: overall structure).

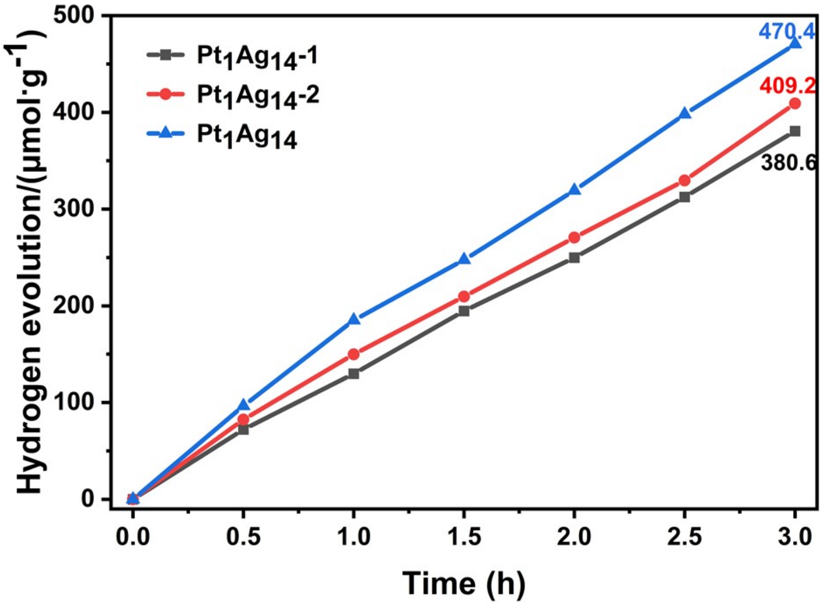

Supplementary Figure 19. Photocatalytic H_2 production of **Pt_1Ag_{14}-1**/g-C_3N_4, **Pt_1Ag_{14}-2**/g-C_3N_4 and **Pt_1Ag_{14}**/g-C_3N_4.

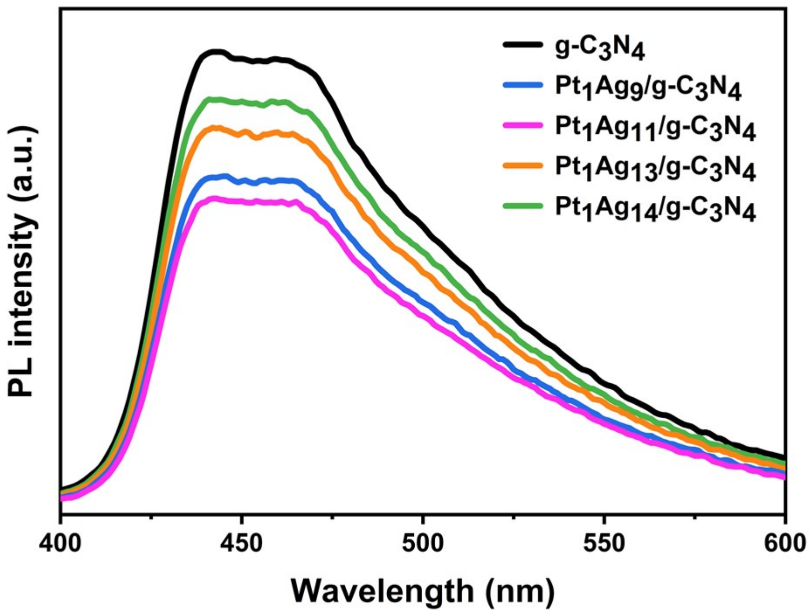

Supplementary Figure 20. Photoluminescence spectra of synthesized g-C_3N_4 and Pt_1Ag_x/g-C_3N_4 (x = 9, 11, 13 and 14).

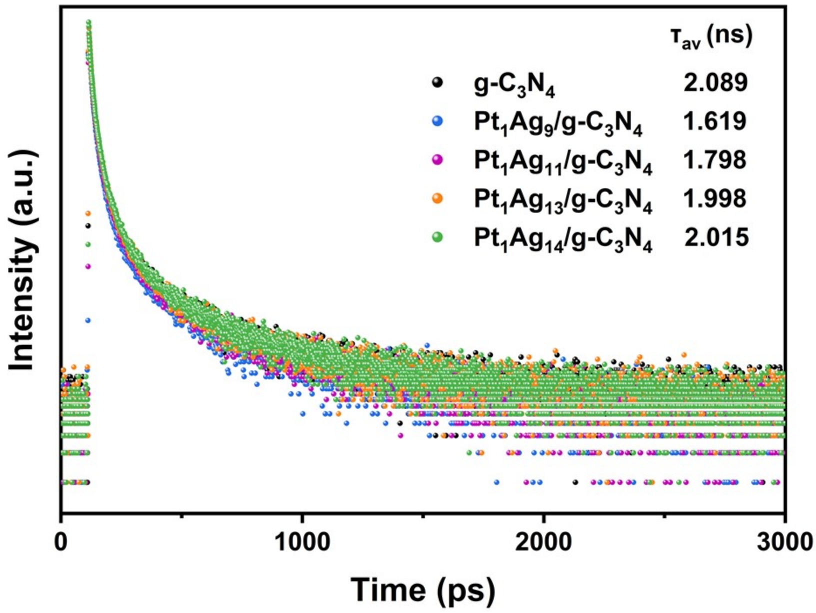

Supplementary Figure 21. Time-resolved PL spectra (λ_{ex} = 373 nm, λ_{em} = 460 nm) of synthesized g-C_3N_4 and Pt_1Ag_x/g-C_3N_4 (x = 9, 11, 13 and 14).

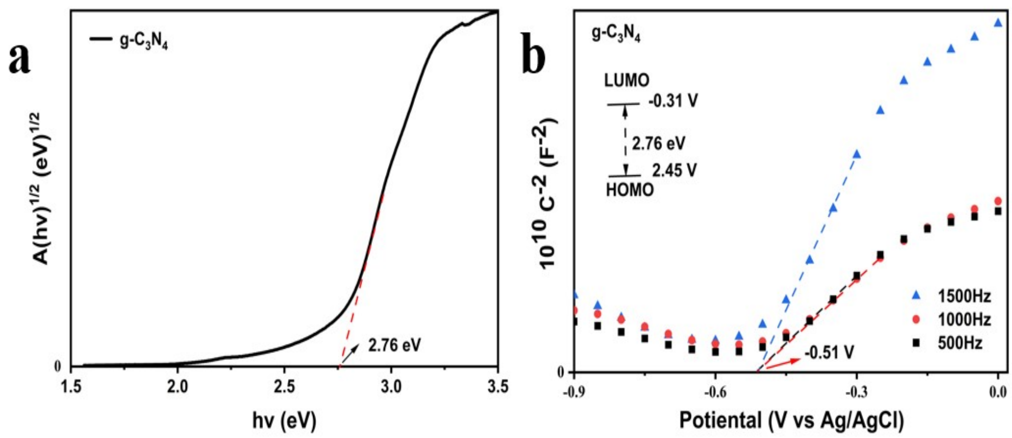

Supplementary Figure 22. (**a**) Tauc plots of g-C_3N_4, (**b**) Mott-Schottky plots of g-C_3N_4 frequency of 500, 1000, and 1500 Hz, respectively (inset: the energy diagram of g-C_3N_4).

The band edge positions of photocatalysis can be calculated using the following equation:

$$E_{CB} = (V\ vs.\ NHE) = E_{fb}\,(V\ vs.\ AgCl/Ag) + 0.197 - X$$

$$E_{VB} = E_{CB} + Eg$$

Where E_{VB} and E_{CB} stand for the valence band edge potential and conduction band edge potential, respectively; $E_{Ag/AgCl}$ = 0.197 V (saturated potassium chloride) vs. NHE; X is the voltage difference between the conduction band value and the flat potential value. In general, the E_{fb} of an n-type semiconductor is approximately equal to the CB potential (E_{CB}).

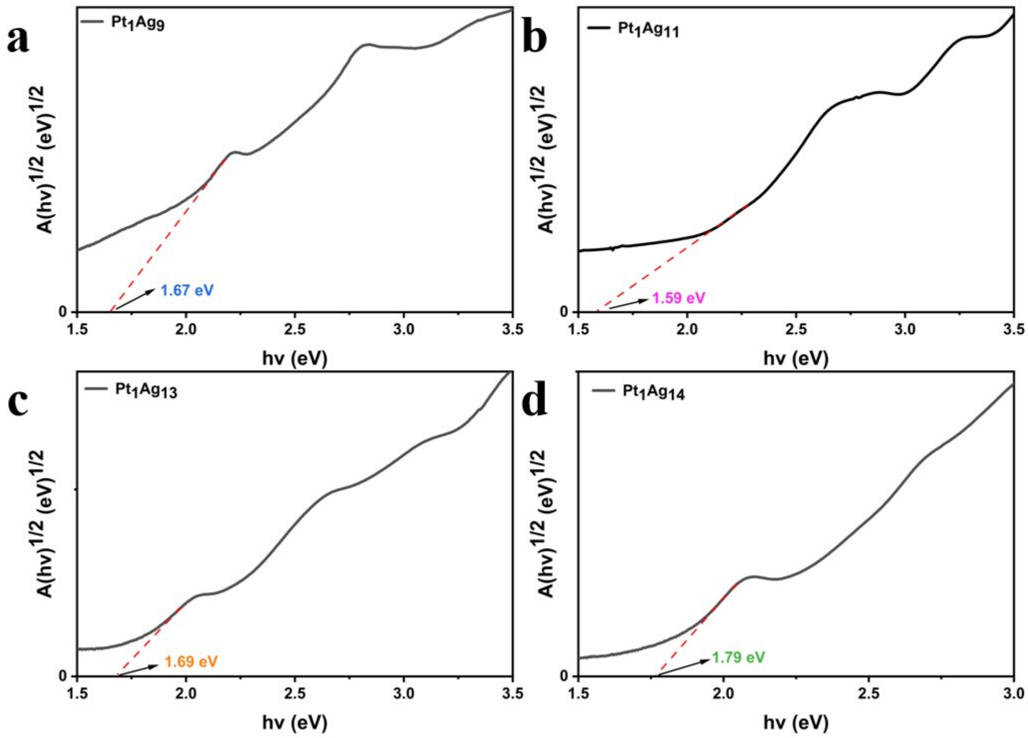

Supplementary Figure 23. Tauc plots of (**a**) Pt_1Ag_9, (**b**) Pt_1Ag_{11}, (**c**) Pt_1Ag_{13} and (**d**) Pt_1Ag_{14}.

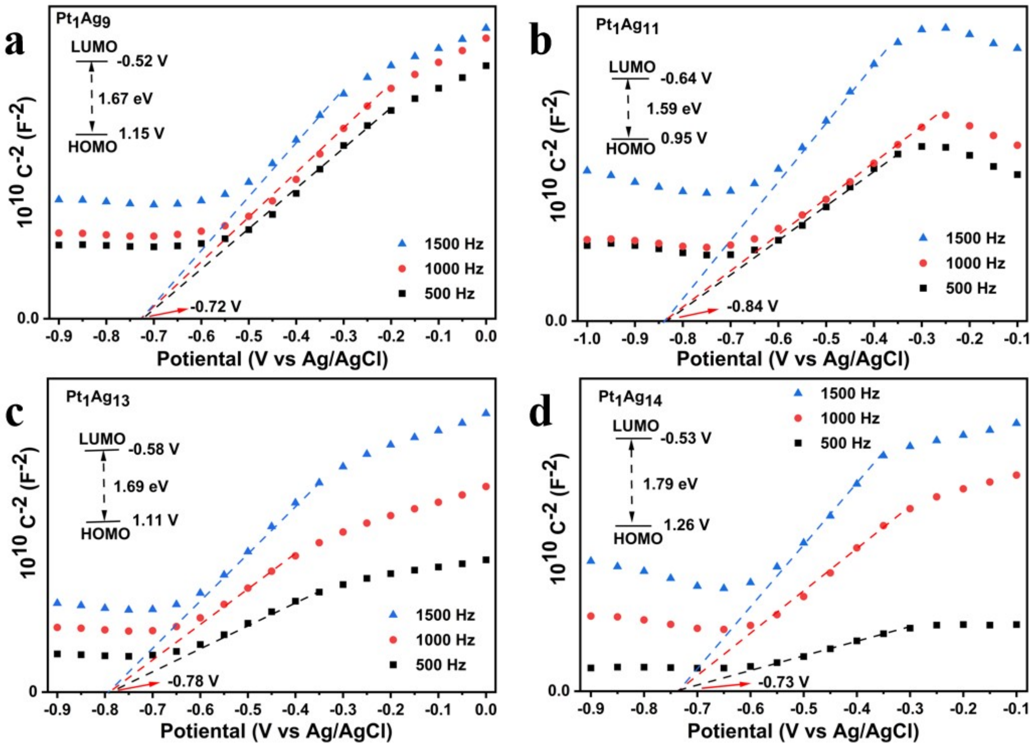

Supplementary Figure 24. Mott-Schottky plots of (**a**) Pt_1Ag_9, (**b**) Pt_1Ag_{11}, (**c**) Pt_1Ag_{13} and (**d**) Pt_1Ag_{14} frequencies of 500, 1000, and 1500 Hz, respectively (inset: the energy diagram of Pt_1Ag_9, Pt_1Ag_{11}, Pt_1Ag_{13} and Pt_1Ag_{14} NCs).

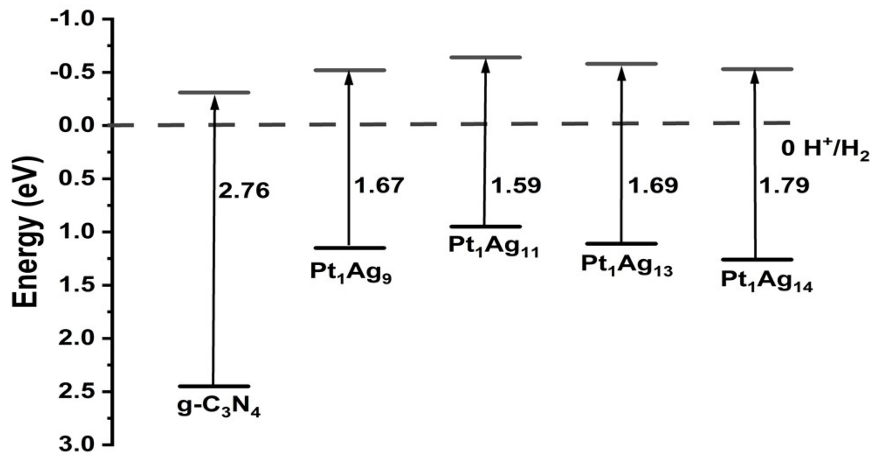

Supplementary Figure 25. Energy diagram of $g\text{-}C_3N_4$ and Pt_1Ag_x NCs (x = 9, 11, 13, and 14).

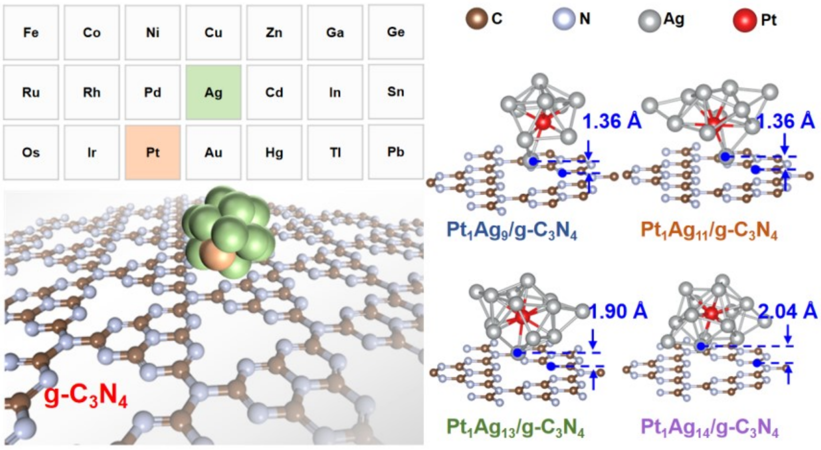

Supplementary Figure 26. Geometric mode for Pt_1Ag_x nanoclusters loaded on g-C_3N_4 monolayer (x = 9, 11, 13, and 14).

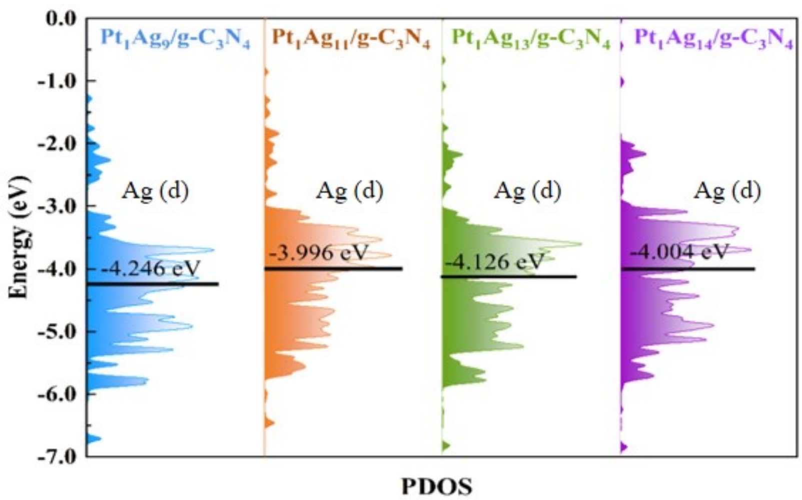

Supplementary Figure 27. The calculated partial densities of states (PDOS) for Pt_1Ag_x/g-C_3N_4. The d-band centers of Ag atoms of Pt_1Ag_x/g-C_3N_4 are labeled (x = 9, 11, 13 and 14). The Fermi level is set to zero.

Supplementary Table 1. Crystal data and structure refinement for the $\mathbf{Pt_1Ag_{11}}$. The CCDC number of $Pt_1Ag_{11}(SR)_5[P(Ph\text{-}p\text{-}OMe)_3]_7$ is 2380779.

Empirical formula	**C179H156Ag11Cl4F20O21P7PtS5**
Formula weight	9847.16
Temperature/K	293(2)
Crystal system	triclinic
Space group	*P-1*
a/Å	19.063(3)
b/Å	19.742(3)
c/Å	27.214(4)
α/°	79.311(12)
β/°	78.555(12)
γ/°	63.042(11)
Volume/Å3	8894(2)
Z	2
ρcalcg/cm3	1.839
μ/mm-1	13.337
F(000)	4852.0
Radiation	CuKα (λ= 1.54186)
2θ range for data collection/°	9.482 to 140.036
Index ranges	-11 ≤ h ≤ 22, -18 ≤ k ≤ 23, -32 ≤ l ≤ 31
Reflections collected	69196
Independent reflections	31583 [Rint = 0.0571, Rsigma = 0.0651]
Data/restraints/parameters	31583/2519/2194
Goodness-of-fit on F2	1.033
Final R indexes [I>=2σ (I)]	R1 = 0.0695, wR2 = 0.1888
Final R indexes [all data]	R1 = 0.0919, wR2 = 0.2059
Largest diff. peak/hole / e Å-3	1.73/-3.07

Supplementary Table 2. The crystal system and space group of Pt_1Ag_x NCs (x = 9, 11, 13, and 14).

Type/NC	Pt_1Ag_9	Pt_1Ag_{11}	Pt_1Ag_{13}	Pt_1Ag_{14}
Crystal system	trigonal	triclinic	triclinic	monoclinic
Space group	*R3*	*P-1*	*P-1*	*C2/c*

Supplementary Table 3. The Bond length data for Pt_1Ag_9 and Pt_1Ag_{11} NCs.

Bond Length(Å) / NC	Pt_1Ag_9	Pt_1Ag_{11}
Pt-Ag	2.7647(2) 2.7646 2.7441 2.7442(2) 2.7323(3)	2.6946 2.7419 2.7256 2.7546 2.7481 2.7131 2.7869 2.7493 2.7687
Ag-Ag	2.9070(3) 2.8192(3) 2.8420(3) 2.8227(3) 2.9596(3) 2.8888(3)	2.8515 2.8557 2.8637 2.8803 2.8071 2.8888 2.8405 2.8796 2.8278 2.7808 2.9513 2.8532 2.8608 2.8991 2.8465 2.8824 2.8517 2.8762
Ag-S	~	2.5749 2.5554 2.4418 2.4535 2.4651 2.4696 2.4530 2.6725 2.6067 2.6274
Ag-P	2.4273(3) 2.4532(3)	2.4338 2.4248 2.4326 2.4852 2.4929 2.4160

Supplementary Table 4. Comparison of angles of Pt_1Ag_9 and Pt_1Ag_{11} NCs.

Angle(°) / NC	**Pt_1Ag_9**	**Pt_1Ag_{11}**
Ag1-Pt-Ag2	64.120	63.231
Ag2-Pt-Ag3	61.965	63.954
Ag3-Pt-Ag4	64.120	61.782
Ag4-Pt-Ag5	61.965	64.190
Ag5-Pt-Ag6	64.120	62.906
Ag1-Pt-Ag6	61.965	62.332
Ag1-Pt-Ag3	117.458	119.793
Ag2-Pt-Ag4	116.401	115.944
Ag3-Pt-Ag5	117.458	116.654
Ag4-Pt-Ag6	116.401	115.903
Ag1-Pt-Ag5	117.458	116.565
Ag2-Pt-Ag6	116.401	116.444

Supplementary Table 5. The Ag and Pt contents in the composite catalysts.

Entry	Sample	Ag content ($*10^{-3}$, wt%)	Pt content ($*10^{-3}$, wt%)
1	$Pt_1Ag_9/g\text{-}C_3N_4$	0.529	0.276
2	$Pt_1Ag_{11}/g\text{-}C_3N_4$	0.611	0.277
3	$Pt_1Ag_{13}/g\text{-}C_3N_4$	0.538	0.268
4	$Pt_1Ag_{14}/g\text{-}C_3N_4$	0.689	0.298

The metal content of nanocomposites can be calculated using the following equation:

$$M \text{ content} = c*v / m; (M=Ag \text{ or } Pt)$$

Where c and *v* stand for the metal consistence and solution volume of ICP-AES testing, respectively; m is sample quality of $Pt_1Ag_x/g\text{-}C_3N_4$ nanocomposites.

Supplementary Table 6. Visible-light photocatalytic hydrogen production activity comparison of a partial of metal clusters/MOF and metal NPs@MOF composites reported.

Photocatalyst	Metal NCs/ NPs	Activity (µmol g-1 h -1)	References
Pt_1Ag_{11}/g-C_3N_4	**Pt_1Ag_{11} NCs**	**1780**	**This work**
Pt/Ce-TTCA	Pt NPs	348.8	*Appl. Catal. B: Environ.* **2021,** *292,* 120156.
Pt/ZSTU-3	Pt NPs	1350	*J. Mater. Chem. A* **2019,** *7,* 11928.
Defect Pt@UiO-66-NH_2-100	Pt NPs	381.2	*Angew. Chem. Int. Ed.* **2019,** *58,* 12175.
Pt/NV-CN	Pt NCs	323.90	*Sep. Purif. Technol.* **2024***, 330,* 125393.
Pt/MIL-125-NH_2/$(OH)_2$	Pt NPs	707	*ACS Appl. Mater. Inter.* **2021,** *13,* 5044.
PtPd cubes @UiO-66-NH_2	PtPd Cubes	697	*Adv. Sci.* **2021,** *8,* 2004456.
CuNPs@d-NH_2-MIL-125	Cu NPs	1326.6	*Chem. Commun.* **2023,** *59,* 8456.
PtNP-MNSs	Pt NPs	317	*Angew. Chem. Int. Ed.* **2019,** *58,* 10198.
Ag_{25}@UiO-66-NH_2	Ag NCs	739.4	*Angew. Chem. Int. Ed.* **2024**, e202401443.
Pt/Cu-MIL-125-NH_2	Pt NPs	490	Angew. Chem. Int. Ed. **2021**, *59*, 1 7182.
Pt-Fc@UiO-66-NH_2	Pt NPs	514.8	Angew. Chem. Int. Ed. **2020**, *60*,16 372.
Pt@TCPP(Mn)⊂DUT-52	Pt NPs	1208	J. Mater. Chem. A **2020**, *8*, 12370.

Supplementary Table 7. Photocatalytic H_2 production of Pt_1Ag_x/g-C_3N_4 (x = 9, 11, 13, and 14).

Materials / Hydrogen production (μmol·g^{-1}·h^{-1})	0.5h	1h	1.5h	2h	2.5h	3h
g-C_3N_4	50.5	54.6	54.3	54.6	53	52.9
Pt_1Ag_{11}	53.4	63.8	79.4	89.4	104.8	113.2
Pt_1Ag_9/g-C_3N_4	292.6	628.4	864.2	1115.2	1308.4	1577.4
Pt_1Ag_{11}/g-C_3N_4	876.2	1780	2798.2	3736.8	4769.4	5731.4
Pt_1Ag_{13}/g-C_3N_4	209.6	448	623	833.8	1050.4	1293.2
Pt_1Ag_{14}-1/g-C_3N_4	72.2	129.7	194.7	249.9	312.6	380.6
Pt_1Ag_{14}-2/g-C_3N_4	82.4	149.8	209.7	270.6	329.6	409.2
Pt_1Ag_{14}/g-C_3N_4	96.4	185.2	247.6	319.2	398	470.4

Supplementary Table 8. Parameters of AQE calculation.

λ (nm)	P ($W \cdot m^{-2}$)	S (10^{-4} m^2)	ν ($\mu mol \cdot h^{-1}$)	ν (10^{-10} $mol \cdot s^{-1}$)	AQE (%)
360	157	1	1.35	3.75	1.59
380	176	1	2.19	6.08	2.18
400	206	1	3.25	9.03	2.62
420	181	1	3.56	9.88	3.11
440	163	1	1.92	5.33	1.78

* The irradiation area was set at 1 cm^2. The glass sealing surface of the reactor was covered with tin foil, and a 1 cm * 1 cm small hole was opened in the center for light transmission.